

Appendix 2

CORRESPONDENCE

Research Correspondence

Magnetic Resonance Imaging-Guided Transcatheter Implantation of a Prosthetic Valve in Aortic Valve Position: Feasibility Study in Swine

Successful transcatheter aortic valve implantation in the aortic valve position has been recently reported (1,2). However, implantation remains challenging, and malpositioning of the device can lead to a life-threatening situation. In contrast to conventional X-ray angiography, magnetic resonance imaging (MRI) provides precise three-dimensional information about both soft tissue anatomy and catheter position as well as immediate parameters of cardiovascular function (3). The purpose of this study was to assess the feasibility of MRI to guide transcatheter valve implantation in the aortic valve position.

Self-expanding, non-covered nitinol stents of 20 mm diameter (Angiomed, Karlsruhe, Germany) were used as a carrier for a prosthetic heart valve. A tricuspid valve was fabricated from a 0.1-mm-thick polytetrafluoroethylene membrane (Impra, Phoenix, Arizona) and sutured into the stent. The valved stent was compressed and front-loaded into a 10-F delivery system that comprised a pig tail and a working lumen. For catheter visualization during MRI, small ferromagnetic markers (size=0.5 mm³) were mounted on the delivery system distally and proximally to the loaded valved stent, comparable to radiopaque markers for conventional X-ray angiography.

Interventions were performed in pigs (n = 7, weight = 26 ± 3 kg) under general anesthesia (2% isoflurane). A 12-F dilator sheath was placed, using Seldinger techniques, in the carotid (n = 4) and iliac artery (n = 3). Thereafter, animals were moved into a 1.5-T MR scanner (Intera, Philips Medical Systems, Best, the Netherlands).

Before intervention, phasic aortic blood flow was measured in the ascending aorta using velocity encoded cine (VEC) MRI (repetition time [TR] = 16 ms, echo time [TE] = 9 ms, field of view [FOV] = 200 to 350, matrix = 256 × 256, phase encoding velocity [V_{enc}] = 200 cm/s). A set of balanced fast field echo (bFFE) images was used to evaluate cardiovascular anatomy including the diameter of the aortic valve annulus and its distance to the coronary artery orifices and the mitral valve. Left ventricular (LV) function (ejection fraction) and biventricular wall motion were assessed in a short-axis plane using standard protocols (TR = 2.7 ms, TE = 1.4 ms, flip angle = 50°, FOV = 200 to 350, matrix = 256 × 256, phases = 20 to 25).

For implantation, the delivery system was advanced from the introducer-sheath to the LV under MR fluoroscopy without use of guide wires. The MR fluoroscopy was based on interactive real-time, steady-state, free processing sequences (TR = 2.7 ms, TE = 1.4 ms, FOV = 200 to 350, matrix = 144 × 144, acquisition frame rate = 10 frames/s; images were displayed online on an in-room monitor, and investigators had hearing protection). Coordinates of the susceptibility markers were taken until the distal marker was seen 2 mm below the aortic valve annulus, and a set of multiphase bFFE images was used to confirm final catheter position. The release of the valved stent was finally monitored under MR fluoroscopy. The aim was to implant the annulus of the prosthetic valve on top of the annulus of the native aortic valve.

After implantation, the following parameters were assessed to determine the success of the intervention: 1) patency of the mitral valve and coronary artery orifices; 2) LV function and biventricular wall motion using bFFE; and 3) phasic aortic blood flow within the lumen of the valved stent using VEC MRI. Finally, the position and morphology of the valved stents were determined at autopsy after the animals were euthanized with pentobarbital.

Paired Student *t* test was used to compare measurements made before and after the intervention and the MRI- and postmortem-derived measurements.

All seven animals had successful implantation of a prosthetic aortic valve without misplacement or cardiovascular trauma. The average duration of the MRI-guided intervention was 53 ± 11 min. Preoperative, bFFE provided clear images for assessment of cardiovascular anatomy (Fig. 1). The diameter of the aortic valve annulus was measured at systole with 17.4 ± 2.1 mm and its distance to the coronary artery orifices and the upper rim of the mitral valve with 10.5 ± 2.8 mm and 8.2 ± 2.7 mm, respectively. At autopsy, measured diameters/distances were 17.8 ± 3.1 mm, 11.1 ± 3.4 mm, and 8.6 ± 2.4 mm, respectively (p = 0.9). The ferromagnetic markers on the shaft of the delivery system produced a circumscribed susceptibility artefact, which was easily perceptible during MRI and enabled clear determination of the position of the loaded valved stent in relation to its surrounding anatomy (Fig. 1).

Susceptibility and radiofrequency shielding effects of the stent allowed quick recognition of the valved stent during and after its delivery but caused no image distortion of the adjacent anatomy (Figs. 1 and 2). After implantation, bFFE images demonstrated the perfusion of the proximal coronary arteries (Fig. 2). Wall motion abnormalities were not observed. The LV ejection fraction as measured before and after valved stent implantation was 61 ± 5% and 60 ± 6%, respectively (p = 0.8). Assessment of quantitative blood flow with VEC MRI showed no aortic regurgitation in five animals and mild central valve incompetence with a regurgitant fraction of 8.2 ± 3.1% in two cases (Fig. 2). There was no evidence for aortic valve stenosis. Peak flow velocities as measured within the lumen of the nitinol stent were 1.1 ± 0.5 m/s compared with 1.0 ± 0.7 m/s measured before the implantation (p = 0.7). Unobstructed mitral valve leaflets were evidenced in all experiments (Fig. 2). Postmortem examination revealed accurate implantation of the prosthetic valve with a precision of 2.3 ± 1.1 mm and confirmed unobstructed coronary arteries (Fig. 2) and mitral valve leaflets.

The current study demonstrates that transcatheter implantation of a prosthetic valve in the aortic valve position is feasible under MRI guidance. The MRI method features the advantage of acquiring images that contain precise three-dimensional information about both soft tissue anatomy and the interventional instrument. Passive MRI catheter tracking by use of susceptibility markers enabled precise position monitoring of the interventional instrument. The 10-F delivery system was easy to control without

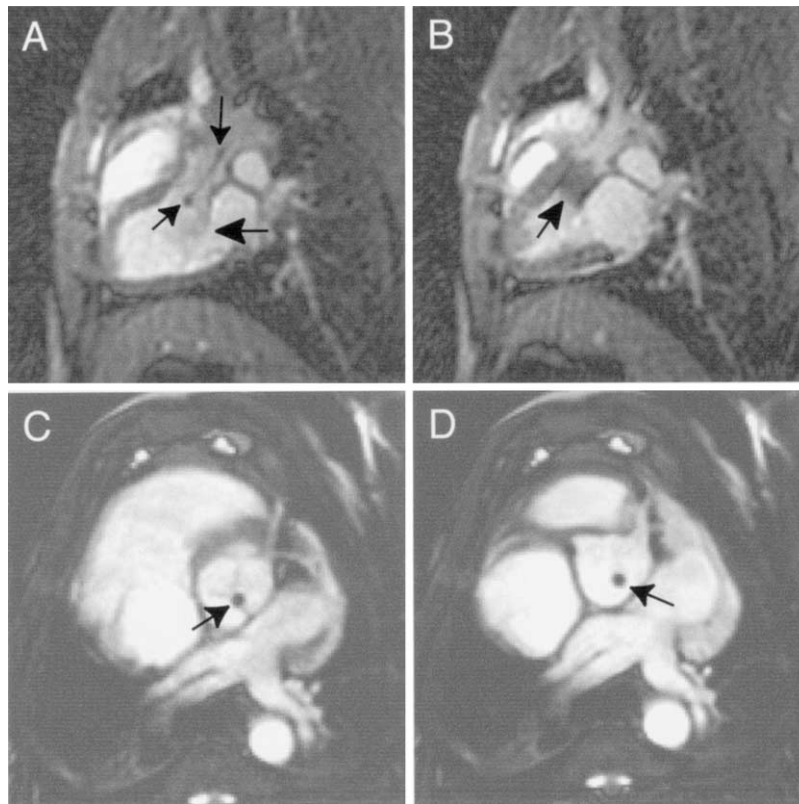


Figure 1. Interactive real-time magnetic resonance image (upper panels) and balanced fast field echo (lower panels) of the heart (swine). Note the susceptibility markers of the delivery system (small arrows in panels A, C, and D), the aortic valve (panel C), coronary arteries (panel D), and mitral valve (large arrow, panel A). Panel B shows the valved stent during delivery (large arrow).

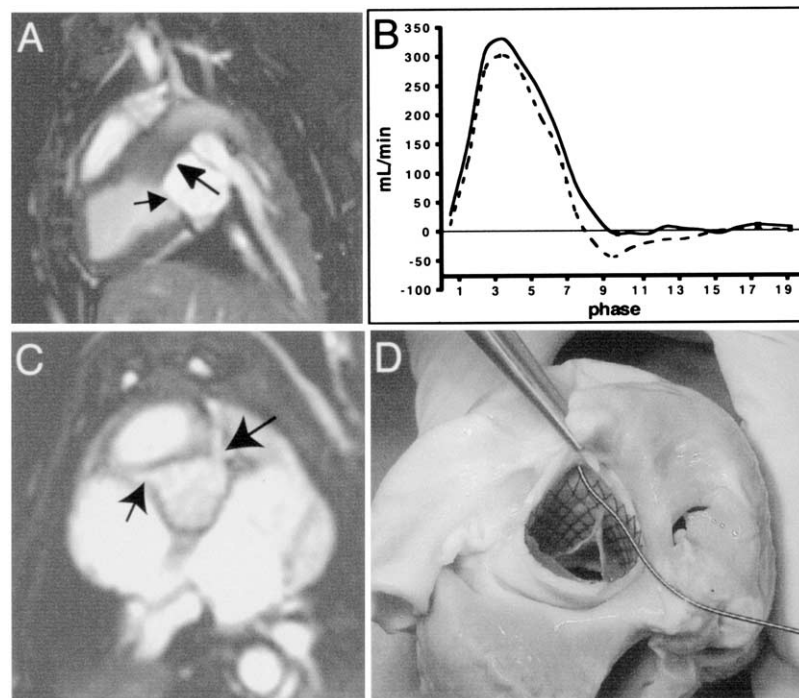


Figure 2. (A) Balanced fast field echo image (bFFE) of implanted valved stent (large arrow) (swine). Note unobstructed mitral valve (small arrow). (B) Representative aortic phasic flow measured with velocity encoded cine MRI within the lumen of a valved stent without (solid line) and with (dotted line) mild aortic insufficiency. (C and D) BFFE image of perfused proximal coronary arteries (arrows) and corresponding photography of the heart with probe within coronary artery.

guide wires. However, the development of guide wires suited for interventional MRI is warranted.

Preoperatively, MRI allowed noninvasive assessment of cardiovascular anatomy and function. During and after implantation, the position of the prosthetic valve was easy to determine. Besides this morphologic information, MRI provided immediate post-intervention physiologic parameters of cardiac function and perfusion of the proximal course of the coronary arteries. In addition, VEC MRI demonstrated optimal function of the implanted prosthetic valve in five cases and mild central valvular insufficiency in two cases.

In conclusion, the results of this study imply that MRI is a promising tool for transcatheter placement of valved stents. However, further validation of safety aspects is needed in chronic studies with larger numbers of animals.

*Titus Kuehne, MD
Sevim Yilmaz, MD
Carolin Meinus, MD
Phillip Moore, MD
Maythem Saeed, DVM, PhD
Oliver Weber, PhD
Charles B. Higgins, MD
Thiemo Blank, PhD
Erhard Elsaesser

Feasibility of Adjusting Paced Left Ventricular Activation by Manipulating Stimulus Strength

To the Editor: Cardiac resynchronization therapy (CRT) improves symptoms and decreases hospitalizations in selected patients with heart failure (1,2). With CRT, pacing from the left ventricle (LV) alters the ventricular activation (VA) sequence, changing the QRS morphology. In responders, change in VA improves cardiac filling and ejection (3). However, many patients are nonresponders. The LV lead location is the major determinant of paced activation but is often constrained by the location of coronary sinus vein branches. During LV mapping for ventricular tachycardia, increased pacing stimulus strength (SS) has been demonstrated to capture an enlarged myocardial area, producing a larger "virtual electrode" (4). If the enlarged area of myocardial capture extends beyond a discrete region of conduction block, the SS increase could result in VA change and more rapid conduction to a remote location, such as the right ventricular (RV) apex.

We hypothesized that paced VA can be manipulated by increasing SS. We expected activation changes to be more marked when pacing near areas of scarred or infarcted myocardium.

Ten patients with New York Heart Association functional class II and III congestive heart failure, ejection fraction <40%, referred for ablation were enrolled according to protocols approved by the Brigham and Women's Hospital human subject protection committee.

Using an electroanatomic mapping system (CARTO, Biosense-Webster Inc., Diamond Bar, California), three-dimensional plots (mean of 136 ± 47 points per patient) of bipolar electrogram amplitude were created (5). Endocardial LV mapping was performed with a 7-F steerable catheter (Biosense-Webster Inc.). Electrograms were recorded on a separate digital system (Prucka Engineering Inc., Houston, Texas). Epicardial mapping by percutaneous subxiphoid approach was performed in one patient. Catheter stability was confirmed by biplane fluoroscopy, the mapping system, and continuous monitoring of electrogram morphology and timing.

Bernhard Schnackenburg, PhD
Peter Ewert, MD
Peter E. Lange, MD
Eike Nagel, MD

*Department of Congenital Heart Diseases
and Pediatric Cardiology
German Heart Institute
Augustenburger Platz 1
Berlin, 13553
Germany
E-mail: titus.kuehne@dhzb.de

doi:10.1016/j.jacc.2004.09.007

REFERENCES

1. Boudjemline Y, Bonhoeffer P. Steps toward percutaneous aortic valve replacement. *Circulation* 2002;105:775-8.
2. Cribier A, Eltchaninoff H, Bash A, et al. Percutaneous transcatheter implantation of an aortic valve prosthesis for calcific aortic stenosis: first human case description. *Circulation* 2002;106:3006-8.
3. Kuehne T, Saeed M, Higgins CB, et al. Endovascular stents in pulmonary valve and artery in swine: feasibility study of MR imaging-guided deployment and postinterventional assessment. *Radiology* 2003;226:475-81.

Pacing at outputs of threshold, 5 mA, and 10 mA was performed at 6 to 10 separated LV sites. In one case, epicardial pacing at 20 mA was performed because of high pacing threshold (10 mA). The anode was in the inferior vena cava (IVC). A quadripolar catheter at the RV apex was the reference catheter. Atrial, ventricular, and His bundle electrograms were assessed to exclude antegrade atrial conduction during pacing.

Stimulus to RV conduction times and stimulus to QRS conduction times (QRS latency) were measured from the stimulus artifact to the first bipolar peak of the electrogram from the RV apical catheter and to the earliest VA in the surface electrocardiogram (ECG). Changes in QRS morphology with pacing were defined as any of the following: QRS width change of >40 ms; new Q-, R-, or S-wave of >25% of the total QRS amplitude; >50% change in ratio of R or S components of QRS complex;

Table 1. Parameters With Stimulus Strength Alteration

	Total	Unchanged QRS	Changed QRS	p Value†
Pacing sites	95	78	17	
Stim to RV (ms)				
Threshold	118 ± 62*	111 ± 52*	150 ± 93	<0.0001
10 mA	95 ± 43	96 ± 43	87 ± 44	
QRS duration (ms)				
Threshold	199 ± 39*	196 ± 40‡	213 ± 28‡	0.03
10 mA	192 ± 43	191 ± 37	195 ± 31	
QRS latency (ms)				
Threshold	47 ± 52*	36 ± 39‡	99 ± 73‡	<0.0001
10 mA	32 ± 34	27 ± 29	54 ± 49	
Electrogram amplitude (mV)	2.0 ± 2.0	2.3 ± 2.1	0.8 ± 1.1	0.007

*p < 0.001 for comparison of threshold with 10 mA stimulus strengths. †p value reported for changed versus unchanged QRS. ‡p ≤ 0.05 for threshold versus 10 mA stimulus strengths.

RV = right ventricle.